Creating structures in polymer blends via a dissolution and phase-separation process

Gavin A. Buxton and Nigel Clarke
Department of Chemistry, University of Durham, Durham, DH1 3LE, United Kingdom
(Received 11 March 2005; published 27 July 2005)

We show how three-dimensional structures can be formed in polymer blends from pre-existing structures. "Tape" of one polymer is inserted into a matrix of an alternative polymer to form an array of parallelepipeds. We subject this regular structure to partial dissolution in the one-phase region, before quenching the system into the two-phase region. The interplay between dissolution and phase separation can result in complex hierarchic structures. In particular, arrays of microchannels of one polymer species can be formed inside the other polymer.

DOI: 10.1103/PhysRevE.72.011807 PACS number(s): 61.41.+e, 82.60.−s

I. INTRODUCTION

The connectivity and complexity inherent to polymer chains can lead to materials with unique, and highly desirable, physical properties. Furthermore, blending two different polymers during processing can result in a solid polymeric material that possesses key properties associated with the individual polymer constituents [1,2]. This offers material scientists the ability to tailor the specific properties of a macroscopic polymer and create optimized compositions. However, different polymer species are generally immiscible and tend to phase separate when mixed. This leads to morphologies where either domains of one polymeric phase are dispersed inside a matrix of the other polymer, or both polymers form bicontinuous domains (an interconnected morphology where both polymeric phases percolate).

The macroscopic properties of polymer blends are often found to be dependent on both the relative concentrations of the different constituents and the morphologies of the blends. Naturally, it is highly desirable to exhibit some control over the morphology of a polymer blend during processing. For example, the application of a shear flow profile during processing can result in highly anisotropic domain structures which lead to anisotropic material properties in the resultant solid polymer [3–5]. The morphologies can also be influenced through *in situ* chemical reactions, where a third polymeric phase is often formed which compatibilizes the different polymeric species [6,7]. Surface wetting phenomena [8–10] or the selective interaction between one of the polymer phases and inclusions (or fillers) [11–13] can also affect a polymer blend morphology. In particular, surface-directed phase separation (where there is a selective affinity between one of the polymers and a solid surface) can result in concentration fluctuations. These fluctuations, or concentration waves, emanate from the solid surface. It should be noted, however, that the patterns formed from surface-directed phase separation are different from those reported here as our initial structures are *not* impenetrable and phase separation (and, hence, pattern formation) occurs throughout the system including regions inside the original structure. Recently, a method for controlling polymer blend morphologies has emerged where the thermodynamic parameters which drive phase separation (temperature, pressure, etc) are varied with time [14–23]. For example, Onuki *et al.* [14,15] elucidated the competition between phase separation and dissolution in systems which are alternatively brought below and above the phase-separation point via periodic temperature variations. However, the simplest and most popular example of phase separation under time-dependent thermodynamic conditions involves "double-quench" conditions. Double quench generally refers to a transition from a one-phase to a two-phase region and a subsequent second quench within the two-phase region. Typically, the second quench is performed such that the driving force for phase separation is increased. The first (shallower) quench results in the formation of separate domains rich in each of the two polymer species. Subsequent to the second (deeper) quench, the shallow domains become unstable and further phase separation occurs *inside* the domains formed during the first quench. Therefore, through the application of double-quench conditions, hierarchic structures consisting of larger domains containing dispersed microdomains can occur [16,17,22,23].

Alternatively, structures can be first dissolved and then quenched by transferring the system from a two-phase region to a one-phase region and, subsequently, back again into a two-phase region. For example, Graca *et al.* [20] considered a three-step process where a PMPS-PS blend was allowed to phase separate in the two-phase region. Once the domain structure was well established, the system was annealed into a one-phase region such that the structure began to dissolve. Prior to complete dissolution the system was brought back into the two-phase region and morphologies similar to that obtained under double-quenched conditions were obtained. Recently, Clarke [21] introduced *pre-existing* particles of one type of polymer into a matrix of a dissimilar polymer. These particles were then allowed to partially dissolve in the one-phase region before the blends were quenched into the two-phase region, such that further phase separation occurred. This provided an alternative method for creating hierarchic structures from prefabricated geometries. Here, we extend this notion by investigating the formation of structures from the annealing and subsequent quenching of three-dimensional structures formed from inserting "tape" of one polymer into the bulk of a dissimilar polymer. These pre-existing structures are assumed to consist of periodic arrays of tape (rectangular parallelepipeds, or cuboids) which extend infinitely in one direction. Through the dissolution (in the one-phase region) and subsequent quenching (in the two-

phase region) of these initial morphologies, we show how three-dimensional hierarchic structures can be obtained.

In order to model the kinetics of the polymer blend dissolution and phase separation, we employ the Cahn-Hilliard method [24,25], modified for polymer blends. The Cahn-Hilliard technique provides an efficient method for capturing the diffusive nature of spinodal decomposition in binary mixtures. This makes the technique particularly applicable to high-viscosity fluids like polymer blends where hydrodynamic interactions can play a negligible role in the evolution of the system. This method has been modified to model the evolution of polymer blends described by the Flory-Huggins free energy of mixing [26]. Furthermore, De Gennes extended the Flory-Huggins theory to include an entropic contribution to the square gradient coefficient which accounts for the chain connectivity of polymer molecules [27]. This modified Cahn-Hilliard method is, therefore, ideal for simulating the phase-separating kinetics of polymer blends.

We use the finite-difference method to computationally evolve the kinetics of the coarse-grained Cahn-Hilliard model; details of this methodology are given in Sec. II. In Sec. III we present our results, and relevant discussions, concerning the construction of three-dimensional structures in polymer blends. We summarize our results and draw conclusions in Sec. IV.

II. METHODOLOGY

We simulate the phase-separation kinetics of an incompressible binary polymer blend using a method which is based on the Cahn-Hilliard model, modified to take into consideration the chain connectivity of polymers. Unless otherwise stated, the three-dimensional systems considered here are of size $L^3=200\times60\times200$, and the systems possess periodic boundary conditions in all three directions [28]. The polymer melt is characterized by the scalar order parameter, ϕ, which represents the concentration of the A-like polymer; the concentration of the B-like polymer is represented by $(1-\phi)$, due to incompressibility constraints. For simplicity, we restrict the current study to symmetric polymer blends in which the degree of polymerization is the same for both the A and B polymers ($N_A=N_B=N$). The kinetic equation describing the evolution of the order parameter is given as [24–26]

$$\frac{\partial\phi}{\partial t}=\nabla\cdot M(\phi)\nabla\frac{\partial F}{\partial\phi}, \tag{1}$$

where $M(\phi)$ is the kinetic coefficient (or mobility) of the order parameter and $F\equiv F\{\phi(\mathbf{r},t)\}$ is the free-energy functional which consists of both local and gradient contributions [29]. The mobility of a polymer species is assumed to be proportional to the concentration of the species. This results in a concentration-dependent mobility of the form, $M(\phi)=D\phi(1-\phi)$ [27,30].

As mentioned earlier, the free-energy functional is composed of both a local and gradient term; the former dictates the energy of mixing and local equilibria, while the latter introduces a surface tension which drives domain growth. The local contribution to the free energy is given by the Flory-Huggins theory to be

$$\frac{F_{FH}}{k_BT}=\int_V\frac{\phi}{N_A}\ln\phi+\frac{1-\phi}{N_B}\ln(1-\phi)+\chi\phi(1-\phi)d\mathbf{r}, \tag{2}$$

where k_B is the Boltzmann constant, T is the temperature, and χ is the Flory-Huggins enthalpic interaction parameter [31,32]. The integration is over the volume of the system. The critical value of the χ parameter at which phase separation occurs in Eq. (2) is given by [26,27]

$$\chi_s=\frac{1}{2}\left(\frac{1}{\phi_0N_A}+\frac{1}{(1-\phi_0)N_B}\right), \tag{3}$$

where ϕ_0 is the average concentration of A-like polymer in the system.

The square gradient term in the free energy is given as [26,27]

$$\frac{F_{dG}}{k_BT}=\int_V\frac{1}{36}\left[\frac{l_A^2}{\phi}+\frac{l_B^2}{1-\phi}\right]|\nabla\phi|^2d\mathbf{r}, \tag{4}$$

where l_i is the Kuhn length of species i, which we currently assume to be the same for both A and B polymers ($l_A=l_B=l$).

Substituting Eqs. (2) and (4) into Eq. (1) can give the following dimensionless (and appropriately scaled) evolution equation [21,26]:

$$\frac{\partial\phi(\mathbf{x},\tau)}{\partial\tau}=\nabla\cdot\phi(1-\phi)\nabla\left[\frac{1}{N|\chi_m-\chi_s|}\ln\frac{\phi}{1-\phi}-\frac{2\chi\phi}{|\chi_m-\chi_s|}+\frac{2\phi-1}{36\phi^2(1-\phi)^2}(\nabla\phi)^2-\frac{\nabla^2\phi}{18\phi(1-\phi)}\right], \tag{5}$$

where $\tau=D(\chi_m-\chi_s)^2t/l^2$ is the dimensionless time scale and $\mathbf{x}=\sqrt{|\chi_m-\chi_s|}\mathbf{r}/l$ is the dimensionless length scale. χ_m is the maximum χ value used during the simulation (the deepest quench). It is straightforward to solve the above equation using the finite difference method (full details are given by Glotzer [26]). In the current study we update the system using a time step of $\Delta\tau=0.02$ and a spatial discretization of $\Delta x=1/\sqrt{8}$. Different step sizes were also studied to ensure that the results were not an artifact of the discretization. The degree of polymerization, $N=2000$, is assumed to be the same for both the A and B polymers. In all the systems considered here, the average concentration is maintained at $\phi_0=0.25$ and spinodal decomposition, therefore, occurs at $\chi>\chi_s=0.001\dot{3}$.

The above model allows us to simulate the kinetics of both the dissolution of the pre-existing structure (at $\chi<\chi_s$) and the subsequent spinodal decomposition from the partially dissolved structure (at $\chi>\chi_s$). Next, we describe results from our three-dimensional investigations into the dissolution and quenching of pre-existing structures and the morphologies that can emerge.

III. RESULTS AND DISCUSSION

Initially we consider a tape of size 10 μm$\times$3 μm$\times\infty$ (or $100\Delta x\times30\Delta x\times\infty$ in lattice units). An order parameter of

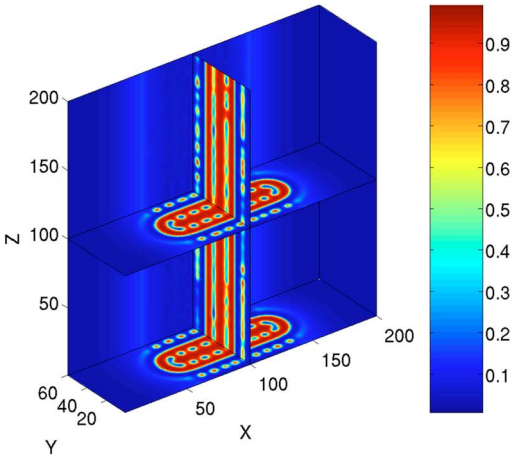

(a)

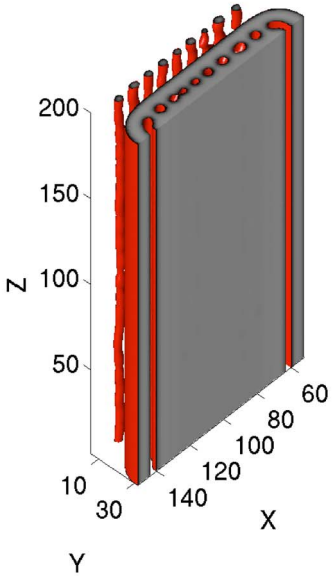

(b)

FIG. 1. (Color online) Snapshot (at time $\tau=2400\Delta\tau$) of a system which has been evolved for $1300\Delta\tau$ at $\chi=0.0001$ prior to the χ parameter being increased to $\chi_m=0.002$. We show both (a) orthogonal contour slices, depicting the concentration of A-like polymers, through the three-dimensional system, and (b) a red isosurface at $\phi=0.5$ with gray-scaled isocaps (regions where A domains cross the system boundaries are shaded between black for $\phi=0.5$ and white for $\phi=1$). Units are dimensionless: see Sec. II for more details.

0.99 is assigned in regions inside the tape volume, while outside the order parameter is 0.01. This order parameter distribution is then perturbed by a Gaussian noise of variance 0.001 and smoothed using a moving average (over nearest neighbors) in order to widen the interfacial width. This preexisting structure is then partially dissolved by evolving the system at $\chi=0.0001$, which is less than $\chi_s=0.001\dot{3}$. At some stage during the dissolution the system is brought within the two-phase region by increasing the χ parameter to χ_m, which is greater than χ_s.

Figure 1 shows a snapshot (at time $\tau=2400\Delta\tau$) of a system which has been evolved for $1300\Delta\tau$ at $\chi=0.0001$ prior

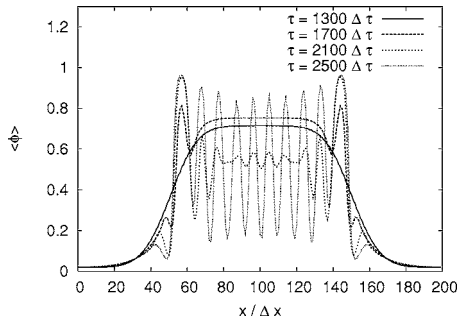

FIG. 2. Average order parameter (averaged over the z direction) for fixed $y=37$, as a function of x. The system shown in Fig. 1 is represented at different times during its evolution. Units are dimensionless: see Sec. II for more details.

to the χ parameter being increased to $\chi_m=0.002$. Figure 1(a) shows orthogonal contour slices, depicting the concentration of A-like polymers, through the three-dimensional system, while Fig. 1(b) shows a red isosurface at $\phi=0.5$ and gray-scaled isocaps (regions where A domains cross the system boundaries are shaded between black for $\phi=0.5$ and white for $\phi=1$). Plotting the data in this manner allows us to gain additional insight into the complex three-dimensional morphologies generated in this study. The tape is initially infinitely extended in the z direction and rectangular in the $x-y$ plane (such that $50<x<150$ and $15<y<45$). Upon the two-step dissolution and quenching process, the system maintains the general aspect ratio of the original structure in the $x-y$ plane. However, the shape of the region has become curved and the sharp rectangular corners are no longer present. Furthermore, during the quenching stage of the two-step process instabilities have arisen both inside the structure and in the neighboring bulk material. This is initially seen as a ring of intermixed ($\phi\approx0.5$) material in the structure and a slight halo of intermixed material around the structure. The intermixed regions coagulate to form a ring of B-polymer channels inside the A-polymer structure and a series of A-polymer channels in the B-polymer matrix. In order to quantify this observation we plot the average order parameter (averaged over the z direction) for fixed $y=37$, as a function of x (see Fig. 2). Therefore, this one-dimensional averaged concentration profile runs through the channels within the polymer structure (see $y=37$ in Fig. 1). We plot the concentration profiles at different times. At time $\tau=1300$ we see the partially dissolved structure prior to quenching the system inside the two-phase region. Quenching the system initially causes strong phase separation to occur at the boundaries of the structure (regions where strong curvature occurs). However, in the center of the system where the channels form, the concentration drops to an intermixed value ($\tau=2100\Delta\tau$) before phase separating into a well-defined and regular periodic pattern ($\tau=2500\Delta\tau$).

A snapshot (at time $\tau=3100\Delta\tau$) of a system which has been evolved for $1800\Delta\tau$ at $\chi=0.0001$ prior to the χ parameter being increased to $\chi_m=0.002$ is shown in Fig. 3. Here, we display orthogonal contour slices through the three-dimensional system. The system was allowed to dissolve for longer than the system shown in Fig. 1. As a consequence of

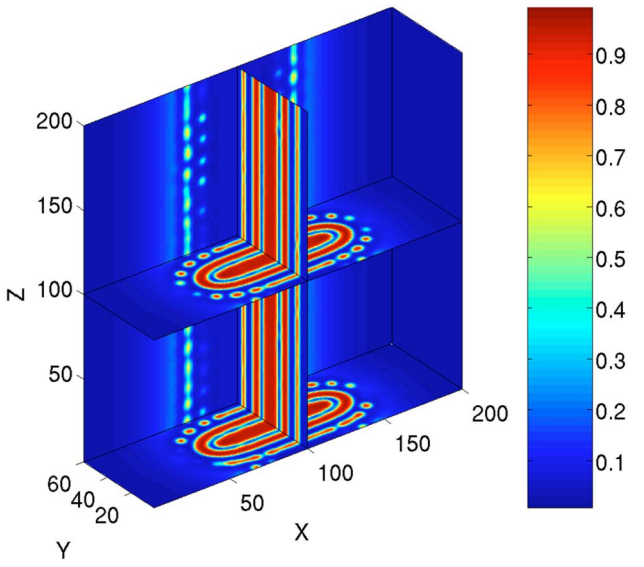

FIG. 3. (Color online) Snapshot (at time $\tau=3100\Delta\tau$) of a system which has been evolved for $1800\Delta\tau$ at $\chi=0.0001$ prior to the χ parameter being increased to $\chi_m=0.002$. We show orthogonal contour slices, depicting the concentration of A-like polymers, through the three-dimensional system. Units are dimensionless: see methodology for more details [34].

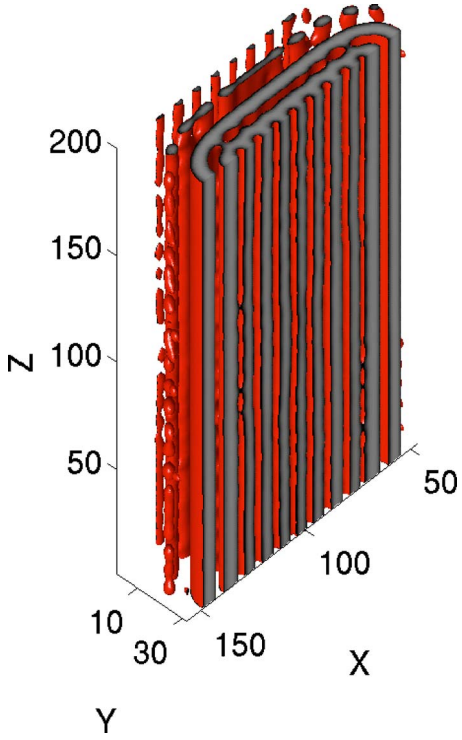

FIG. 4. (Color online) Snapshot (at time $\tau=3000\Delta\tau$) of a system which has been evolved for $2000\Delta\tau$ at $\chi=0.0001$ prior to the χ parameter being increased to $\chi_m=0.002$. We show a red isosurface at $\phi=0.5$ with gray-scaled isocaps (regions where A domains cross the system boundaries are shaded between black for $\phi=0.5$ and white for $\phi=1$). Units are dimensionless: see Sec. II for more details [34].

this greater dissolution, a ring of intermixed material again appears in the structure, but now phase separates to form a band of continuous B-rich polymer. This essentially results in a region of A-like polymer, much smaller than the original tape size, surrounded by a band of B-like polymer, which is itself enclosed in a band of A-like polymer. The size of this outer band is closer to the original size of the tape structure. Furthermore, the channels of A-like polymer which form in neighboring regions of the bulk B-like polymer appear to coagulate slightly around the central regions ($x\approx100$).

A further increase in the time at which the original tape structure is allowed to dissolve, before the system is quenched into the two-phase region, is shown in Fig. 4. We depict a system at time $\tau=3000\Delta\tau$ which has been evolved for $2000\Delta\tau$ at $\chi=0.0001$ prior to the χ parameter being increased to $\chi_m=0.002$. There are several effects of this further dissolution, in particular the formation of a series of channels in the center of the structure. To highlight this particular feature we represent the data as an isosurface which depicts the interface between A-rich and B-rich domains. Dissolving and quenching the system now leads not only to a band of intermixed material forming within the confines of the original structure, but also intermixed material forming in the center of the structure. These intermixed regions phase separate to form not only a band of B-like polymer inside the structure, but also an array of B-like polymer microchannels in the center of the structure.

Figure 5 elucidates the formation of the central microchannels shown in Fig. 4. The average order parameter (averaged over the z direction) for fixed $y=30$ is plotted as a function of distance in the x direction. The one-dimensional profiles run through the center of the simulation and reveal the formation of the central channels. We see that the phase-separation process is initially instigated at the boundaries (where the system is curved) and proceeds through the system towards the center. At time $\tau=3000\Delta\tau$ we see that a regular array of several microchannels forms within the center of the structure.

We can also obtain additional insight into the complexity of these systems by considering the interfacial area, A_I, as a function of time (calculated using the "broken bond method" [33]). See Fig. 6. The interfacial area is inversely proportional to the domain size, and we shift the time scale by τ_Q, the time at which quenching occurs. For the system which is allowed to evolve for $700\Delta\tau$ prior to quenching (τ_Q

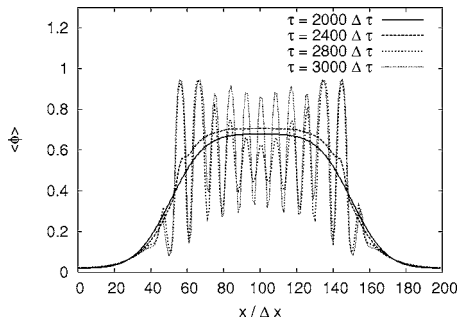

FIG. 5. Average order parameter (averaged over the z direction) for fixed $y=37$, as a function of x. The system shown in Fig. 4 is represented at different times during its evolution. Units are dimensionless: see Sec. II for more details.

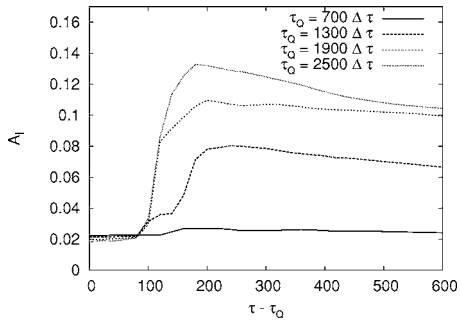

FIG. 6. Interfacial area as a function of time for systems quenched from the one-phase region (χ=0.0001) into the two-phase region (χ_m=0.002) after different times. Units are dimensionless: see Sec. II for more details.

=700$\Delta\tau$), the system possesses little variation as a function of time. The structure that forms after quenching resembles the original tape structure, although the "corners" of the rectangular structure become smoothed and slight phase separation occurs in the tape structure towards the edges. As the time prior to quenching, τ_Q, is increased, the systems are allowed to dissolve for longer and, hence, more interesting structures emerge. As can be seen from Figs. 1–5, the effect of increasing τ_Q causes a ring of *B*-like channels to be formed in the *A*-like structure and eventually, at $\tau_Q > 2000\Delta\tau$, a band of *B*-like material with a central region of microchannels. This increasing complexity can be seen to result in the formation of greater interfacial area.

We next turn our attention from the effects of varying the duration of dissolution to the effects of varying the quench depth. The system is allowed to dissolve for $2000\Delta\tau$ before the system is brought within the two-phase region ($\chi \rightarrow \chi_2$). During the course of these runs $|\chi_m - \chi_s|$ [see Eq. (5)] is maintained at $|0.0024 - 0.0013\dot{}|$, where χ_m is the maximum χ value used during these runs, thus maintaining the same spatial and temporal scales and discretization. The effects of varying χ_m is depicted in Fig. 7. Figure 7(a) shows an isosurface plot of the concentration fluctuations in the system with χ_2=0.0015, at time $\tau=5000\Delta\tau$. If this system is contrasted with Fig. 7(b), which shows the same system but with χ_2=0.0024, we see a difference in the complexity of the patterns formed. The driving force for phase separation is reduced for lower χ values and, therefore, systems which undergo a shallower second quench are allowed to diffuse more prior to phase separation and the formation of complex structures. The instabilities in the *A*-rich and *B*-rich regions of the system (subsequent to thrusting the system into the two-phase region) are allowed to diffuse prior to phase separation. In the systems presented in Fig. 7(b), the quench is deeper and, therefore, phase separation occurs faster and structures of greater complexity are formed.

Further insight into this phenomenon is given in Fig. 8, which depicts the interfacial area as a function of time for systems quenched to different depths. The level of interfacial area is dramatically increased as the complexity of the patterns formed increases. The system of χ_2=0.0015 maintains a structure similar to that of the dissolved tape as the system gradually comes out of solution. Hence, the interfacial area shows little variation. As the χ parameter is increased the amount of time prior to the formation of a structure is shorter

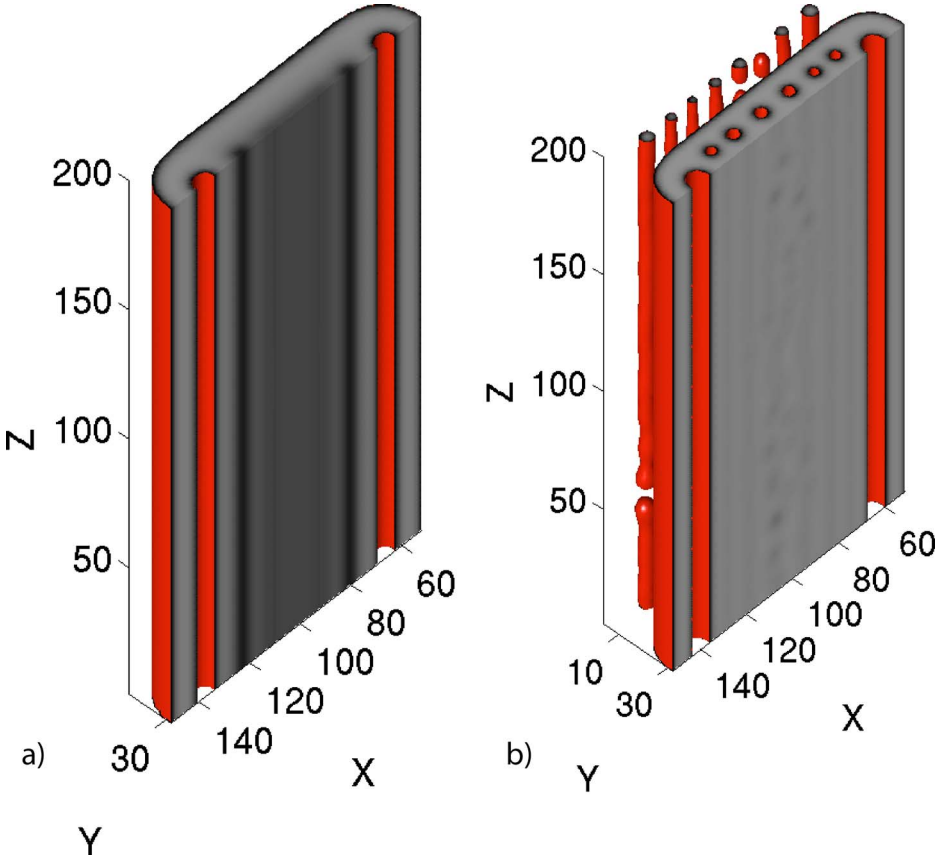

FIG. 7. (Color online) Snapshots (at time $\tau=5000\Delta\tau$) of two systems which have evolved for $2000\Delta\tau$ at χ=0.0001 prior to the χ parameter being increased to (a) χ_2=0.0015 and (b) χ_2=0.0024. Red isosurfaces at ϕ=0.5 with gray-scaled isocaps (regions where *A* domains cross the system boundaries are shaded between black for ϕ=0.5 and white for ϕ=1) are shown. Units are dimensionless: see Sec. II for more details.

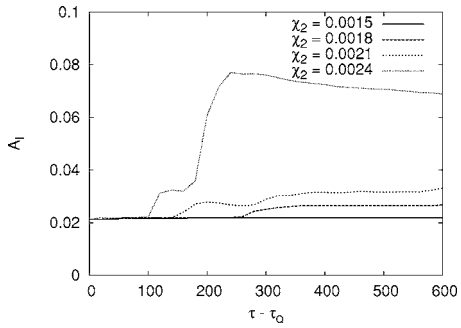

FIG. 8. Interfacial area as a function of time for systems quenched from the one-phase region (χ=0.0001) into the two-phase region after a time of τ=2000$\Delta\tau$. Different quench depths are contrasted. Units are dimensionless: see Sec. II for more details.

and the complexity of the structures (magnitude of the interfacial area) is increased.

Finally, we turn our attention to the effects of aspect ratio. In all the systems considered so far we assumed that the tape was 10 μm$\times$3 μm$\times\infty$ in size, in a system of size 20 μm $\times$6 μm$\times\infty$ (such that ϕ_0=0.25). Here, we vary the aspect ratio of the initial tape structure by varying the size in the x direction, maintaining, however, a ratio between system length and tape length of 2. In this manner, ϕ_0 is maintained at 0.25. We evolve the systems for 2000$\Delta\tau$ at χ=0.0001 prior to increasing the χ parameter to χ_m=0.002. A snapshot, at a time τ=3000$\Delta\tau$, of the structure obtained for an initial tape of size 6 μm$\times$6 μm$\times\infty$ is shown in Fig. 9, which shows an isosurface plot which depicts the interface between A-rich and B-rich domains. The system evolves into a structure consisting of a central column of A-like polymer surrounded by rings of both B-like and A-like polymer, respectively. Also present are isolated columns of A-like polymer in the neighboring bulk material. We quantify the evolution of this structure in Fig. 10, which depicts the average order parameter (averaged over the z direction and considering y =30, through the center of the simulation) as a function of x at various times during the simulation. Initially the concentration of A-like polymer is diffuse and spreads out over a wide region. Upon quenching, the system evolves to reveal the structure depicted in Fig. 9 at time τ=3000$\Delta\tau$. The central region of A-like polymer in the center of the column at time τ=3000$\Delta\tau$ diffuses out to the surrounding A-like polymer ring to form a central channel of B-like polymer and a "sheath" of A-like polymer (e.g., at time τ=4000$\Delta\tau$).

Figure 11 shows orthogonal contour slices through a system with an initial tape of size 15 μm$\times$3 μm$\times\infty$ at time τ=3000$\Delta\tau$. The morphologies obtained are similar to that shown in Fig. 4 (which shows a system initially containing a tape of size 10 μm$\times$3 μm$\times\infty$). Morphologies emerge which consist of an array of channels rich in B-like polymer in the center of the structure. The evolution of this system is further examined in Fig. 12, which considers the average order parameter as a function of distance in the x direction (averaged over the z direction and considering y=30, through the center of the simulation). The formation of the complex structure is again seen to initiate at the edges of the structure and results in an array of microchannels throughout

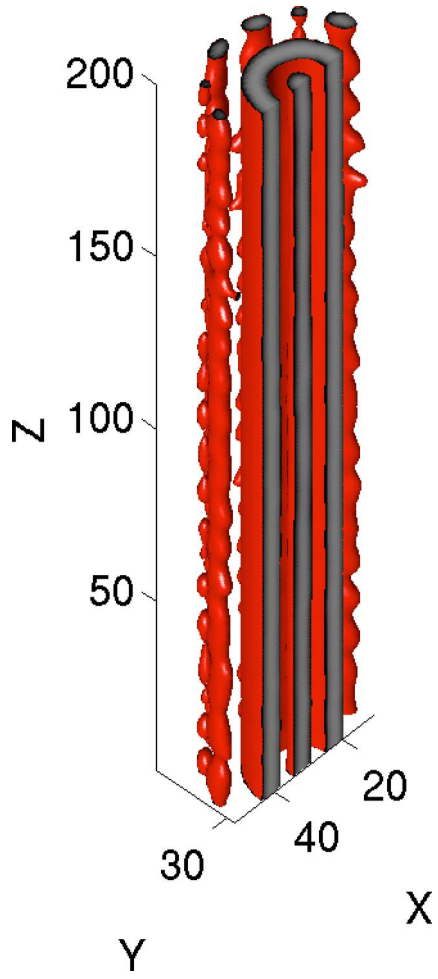

FIG. 9. (Color online) Snapshot (at time τ=3000$\Delta\tau$) of a system initially containing a tape of size 6 μm$\times$6 μm$\times\infty$ which has been evolved for 2000$\Delta\tau$ at χ=0.0001 prior to the χ parameter being increased to χ_m=0.002. We show a red isosurface at ϕ=0.5 with gray-scaled isocaps (regions where A domains cross the system boundaries are shaded between black for ϕ=0.5 and white for ϕ =1). Units are dimensionless: see Sec. II for more details [34].

the sample. The fine array of microchannels diffuses out with time, as the domains grow and coarsen, and at time τ =4000$\Delta\tau$ this internal structure is no longer present.

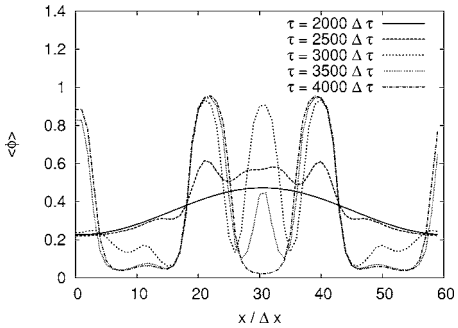

FIG. 10. Average order parameter (averaged over the z direction) for fixed y=30, as a function of x. The system shown in Fig. 9 is represented at different times during its evolution. Units are dimensionless: see Sec. II for more details.

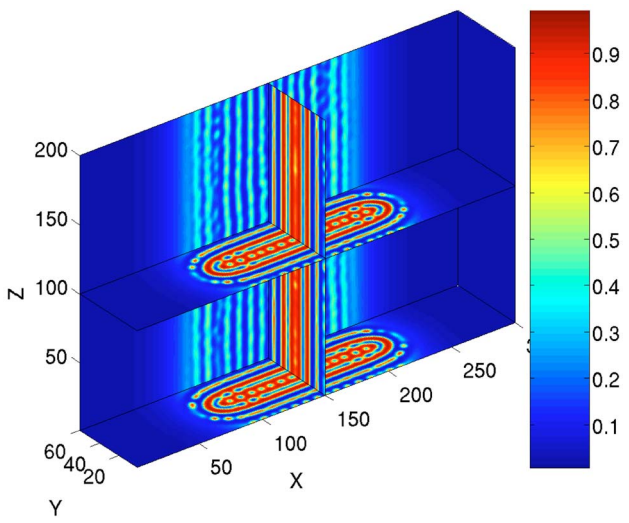

FIG. 11. (Color online) Snapshot (at time $\tau=3000\Delta\tau$) of a system initially containing a tape of size 15 μm$\times$6 μm$\times\infty$ which has been evolved for $2000\Delta\tau$ at $\chi=0.0001$ prior to the χ parameter being increased to $\chi_m=0.002$. We show orthogonal contour slices, depicting the concentration of A-like polymers, through the three-dimensional system. Units are dimensionless: see Sec. II for more details [34].

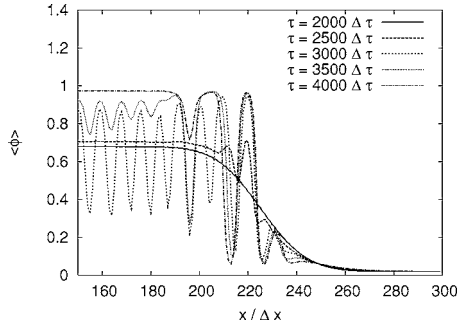

FIG. 12. Average order parameter (averaged over the z direction) for fixed $y=30$, as a function of x. The system shown in Fig. 11 is represented at different times during its evolution. Units are dimensionless: see Sec. II for more details.

IV. SUMMARY AND CONCLUSIONS

We have demonstrated that the dissolution and quenching of pre-existing morphologies can lead to various structures. These structures are formed from inserting a regular array of A-like polymer tape structures into a matrix of B-like polymer. These initial structures are then allowed to dissolve in the one-phase region ($\chi<\chi_s$). Prior to complete dissolution the system is brought into the two-phase region ($\chi>\chi_s$). This process is shown to produce interesting structures. In particular, the complexity of the structures is found to increase with increasing duration of dissolution and increasing quench depth.

The structures presented here are not only of scientific interest, but could also have technological importance. For example, if the A-like polymer phase shown in Fig. 9(b) was conductive (or reinforced with conducting nanoparticles), then the structure might well resemble a coaxial cable, with the central A-like polymer column, comprising the inner wire, being separated by the B-like polymer ring from the outer A-like polymer ring, which would act as the screening wire. It is, therefore, highly desirable to control the formation of hierarchical structures in polymer blends and, thereby, isolate potential technologically important morphologies.

[1] *Polymer Blends*, edited by D. R. Paul and C. B. Bucknall (Wiley, New York, 2000).
[2] G. R. Strobl, *The Physics of Polymers* (Springer-Verlag, Berlin, 1996).
[3] T. Ohta, H. Nozaki, and M. Doi, J. Chem. Phys. **93**, 2664 (1990).
[4] F. Corberi, G. Gonnella, and A. Lamura, Phys. Rev. Lett. **81**, 3852 (1998).
[5] G. A. Buxton and A. C. Balazs, Phys. Rev. B **69**, 054101 (2004).
[6] S. C. Glotzer, E. A. DiMarzio, and M. Muthukumar, Phys. Rev. Lett. **74**, 2034 (1995).
[7] K. Good, O. Kuksenok, G. A. Buxton, V. V. Ginzburg, and A. C. Balazs, J. Chem. Phys. **121**, 6052 (2004).
[8] P. Guenoun, D. Beysens, and M. Robert, Phys. Rev. Lett. **65**, 2406 (1990).
[9] R. A. L. Jones, L. J. Norton, E. J. Kramer, F. S. Bates, and P. Wiltzius, Phys. Rev. Lett. **66**, 1326 (1991).
[10] G. Brown and A. Chakrabarti, Phys. Rev. A **46**, 4829 (1992).
[11] G. Peng, F. Qui, V. V. Ginzburg, D. Jasnow, and A. C. Balazs, Science **288**, 1802 (2000).
[12] A. Karim, J. F. Douglas, G. Nisato, D.-W. Liu, and E. J. Amis, Macromolecules **32**, 5917 (1999).
[13] B. P. Lee, J. F. Douglas, and S. C. Glotzer, Phys. Rev. E **60**, 5812 (1999).
[14] A. Onuki, Phys. Rev. Lett. **48**, 753 (1982).
[15] M. Joshua, W. I. Goldburg, and A. Onuki, Phys. Rev. Lett. **54**, 1175 (1985).
[16] H. Tanaka, Phys. Rev. E **47**, 2946 (1993).
[17] J. Tao, M. Okada, T. Nose, and T. Chiba, Polymer **36**, 3909 (1995).
[18] T. Hashimoto, M. Hayashi, and H. Jinnai, J. Chem. Phys. **112**, 6886 (2000).
[19] M. Hayashi, H. Jinnai, and T. Hashimoto, J. Chem. Phys. **112**, 6897 (2000).
[20] M. Graca, S. A. Wieczorek, and R. Holyst, Macromolecules **35**, 7718 (2002).
[21] N. Clarke, Phys. Rev. Lett. **89**, 215506 (2002).
[22] T. Sigehuzi and H. Tanaka, Phys. Rev. E **70**, 051504 (2004).
[23] I. C. Henderson and N. Clarke, Macromolecules **37**, 1952 (2004).
[24] J. W. Cahn and J. E. Hilliard, J. Chem. Phys. **28**, 258 (1958).
[25] J. W. Cahn, J. Chem. Phys. **42**, 93 (1965).
[26] S. C. Glotzer, Annu. Rev. Comput. Phys. **2**, 1 (1995).

[27] P. G. de Gennes, J. Chem. Phys. **72**, 4756 (1980).
[28] We note that the behavior of the systems was not greatly affected by the boundary conditions used. The structures were the same, at least during the time scales considered here, for no-flux boundary conditions and systems where the box size was increased (decreasing χ_s globally, but not locally).
[29] The "Cookean" noise term is neglected from the current study. This term, however, has been found to have little effect on the domain growth of simple fluids and is often omitted from polymeric studies for computational reasons. See Glotzer (Ref. [26]) for more details.
[30] F. Brochard, J. Jouffroy, and P. Levinson, Macromolecules **16**, 1638 (1983).
[31] M. L. Huggins, J. Am. Chem. Soc. **64**, 1712 (1942).
[32] P. J. Flory, *Principles of Polymer Chemistry* (Cornell University Press, New York, 1953).
[33] T. Ohta, D. Jasnow, and K. Kawasaki, Phys. Rev. Lett. **49**, 1223 (1982).
[34] See EPAPS Document No. PLEEE8-72-012508 for alternative depictions of Figs. 3, 4, 9, and 11. This document can be reached via a direct link in the online article's HTML reference section or via the EPAPS homepage (http://www.aip.org/pubservs/epaps.html).